

Abstract

Mobile Differential Optical Absorption Spectroscopy measurements of SO₂ and NO₂ were performed in the Guangzhou Eastern Area (GEA) during the Guangzhou Asian Games 2010 from November 2010 to December 2010. Spatial and temporal distributions of SO₂ and NO₂ in this area were obtained and emission sources were determined by using wind field data. The NO₂ vertical column densities were found to agree with OMI values. The correlation coefficient (R^2) was 0.88 after cloud filtering. During the Guangzhou Asian Games and Asian Paralympics (Para) Games, the SO₂ and NO₂ emissions in the area were quantified using averaged wind speed and wind direction. For times outside the Games the average SO₂ emission was estimated to be 9.50 ± 0.90 tons per hour and the average NO₂ emission was estimated to be 3.50 ± 1.89 tons per hour. During the phases of the Asian and Asian Para Games, the SO₂ and NO₂ emissions were reduced by 53.5 and 46%, respectively, compared to the usual condition. We also investigated the influence of GEA on Guangzhou University Town, the main venue located northwest of the GEA, and found that SO₂ concentrations here were about tripled by emissions from the GEA.

1 Introduction

NO₂ is an important trace gas in the atmosphere because it readily undergoes photochemical reactions with other air pollutants. High NO₂ levels, however, are a health risk. For example, long-term exposure to NO₂ increases the symptoms of bronchitis in asthmatic children (WHO, 2006). The major sources of anthropogenic emissions of NO₂ are combustion processes such as heating, power generation, and engines in vehicles and ships (Finlayson-Pitts et al., 1999). SO₂ is a colorless gas that adversely affects the respiratory system, especially the lungs. The main anthropogenic source of SO₂ is the burning of sulfur-containing fossil fuels for domestic heating and power

Observations of SO₂ and NO₂ by mobile DOAS in Guangzhou Eastern Area

F. C. Wu et al.

Title Page

Abstract

Introduction

Conclusions

References

Tables

Figures

◀

▶

◀

▶

Back

Close

Full Screen / Esc

Printer-friendly Version

Interactive Discussion



generation. SO₂ and NO₂ tend to form sulfuric and nitric acids, respectively, which in the form of acid rain, are one of the causes of deforestation (WHO, 2006).

Population growth, industrial development, and heavy traffic lead to higher energy consumption and, therefore, an increasing in the emission of pollutants such as SO₂, NO₂, and Volatile Organic Compounds (VOCs) into the atmosphere. In recent years, China has experienced a significant increase in atmospheric pollutant concentrations because of rapid industrial development, which has an important impact on ecosystems and human health. The Pearl River Delta (PRD) in the south of China is one of the three major economic areas (the other two are the Yangtze River Delta and the Beijing-Tianjin-Hebei Economic region). It includes many populated and strongly industrialized cities such as Guangzhou and Shenzhen, and has experienced an extremely fast economic development (Zhang et al., 2008a,b; Wang et al., 2008). PRD has a total land area of 42 794 km² and a population of over 38 million (Cao et al., 2004). As a result, emissions of SO₂, NO₂, and other pollutants have also largely increased in this area (Zhang et al., 2007).

The 16th Asian Games was held in the city of Guangzhou from November 2010 to December 2010. The pollutant sources were identified in order to alleviate air pollution for this occasion. In addition, strategies including emission control for factories, vehicle limitation, and so forth were employed by the Guangzhou government to reduce the air pollution problem during the Asian Games. The Guangzhou Eastern Area (GEA) (Fig. 1) was considered the most seriously affected region of the city because of the many pollutant sources present, such as the Guangdong Yuehua Power Plant (the largest power plant in Guangzhou according to the Guangzhou Environmental Center), the Guangzhou Hengyun Thermal Power Company, and the Guangzhou Zhujiang Steel Company, where air pollutants such as SO₂, NO₂, VOCs, and fine particulates are emitted. Regional studies investigated that area sources have a very strong influence on air quality through the regional transport of air pollutants, possibly causing severe pollution events to the area and its neighbors (Melamed et al., 2009; Takashima et al., 2011). The temporal and spatial scale of transportation can range from a few days to several

Observations of SO₂ and NO₂ by mobile DOAS in Guangzhou Eastern Area

F. C. Wu et al.

Title Page

Abstract

Introduction

Conclusions

References

Tables

Figures

⏪

⏩

◀

▶

Back

Close

Full Screen / Esc

Printer-friendly Version

Interactive Discussion



Observations of SO₂ and NO₂ by mobile DOAS in Guangzhou Eastern Area

F. C. Wu et al.

[Title Page](#)[Abstract](#)[Introduction](#)[Conclusions](#)[References](#)[Tables](#)[Figures](#)[⏪](#)[⏩](#)[◀](#)[▶](#)[Back](#)[Close](#)[Full Screen / Esc](#)[Printer-friendly Version](#)[Interactive Discussion](#)

weeks and from a few kilometers to hundreds of kilometers. Therefore, understanding the spatial and temporal distribution as well as the emission sources of air pollutants in GEA was important for environmental management during the Guangzhou Asian Games. Air pollutants were routinely monitored by the local environmental protection agency using a network of ground-level monitors. Data from this network were insufficient for spatial distribution and transportation processes as well as emission sourcing.

Previously, regional studies in the PRD combined aircraft measurements and models to examine spatial and vertical distributions of O₃, SO₂, NO_x, PM₁₀, and PM_{2.5} (Wang et al., 2008) or used a bottom-up approach to estimate emissions of NO_x, SO₂, CO, VOCs, and fine particulates (Zheng et al., 2009; He et al., 2011). These studies focused on the larger area of the PRD but did not consider smaller-scale distributions of air pollutants or area sources like the GEA. In this study, Differential Optical Absorption Spectroscopy (DOAS) on a mobile platform was used to detect spatial and temporal distributions and emissions of SO₂ and NO₂ related to the GEA. This technique was first used to measure volcanic emissions (Edner et al., 1994; Galle et al., 2003) and subsequently applied to determine the emission of point sources (e.g. power plants, oil refineries, etc.) and area sources (e.g. cities and industrial areas). Johansson et al. (2008, 2009) and Rivera et al. (2009) examined the outflow of SO₂, NO₂, and HCHO in Mexico, Beijing and the Tula industrial area. NO_x emissions in Mannheim and Ludwigshafen using mobile MAX-DOAS (Multi-Axis Differential Optical Absorption Spectroscopy, MAX-DOAS) were investigated by Ibrahim et al. (2010). The same method was used by Shaiganfar et al. (2011) to quantify emissions in Delhi. In China, several measurements based on mobile DOAS were also carried out (Li et al., 2005, 2007b; Wu et al., 2011). However, in previous field measurements that used a zenith viewing DOAS instrument on a mobile platform, emissions were estimated by first taking a “clean-air” spectrum at some point along the measurement path and using it as a reference spectrum to obtain differential vertical columns relative to this “clean-air” measurement (Li et al., 2005, 2007b; Wu et al., 2011). For the field campaign reported in the present study, concurrent measurements of a MAX-DOAS instrument at a fixed

only allowed to drive on odd days from 1 November to 29 November and from 5 to 21 December 2010, whereas vehicles with even number plates were allowed only on even days. Our van has an odd number plate; therefore, we had a total of 25 days of measurements. During the entire measurement period, the temperature varied from 22 °C to 28 °C, and the wind blew predominantly from the north/northeast (see Sect. 3.1.1 for further details).

2.2 Description of the instrument

Our mobile DOAS instrument records sunlight scattered into the telescope pointing to the zenith. A schematic diagram of the mobile DOAS system developed at the Anhui Institute of Optics and Mechanics (AIOFM) is shown in Fig. 2. The components of our AIOFM mobile DOAS instrument are the telescope, a UV/VIS detector spectrometer unit, a computer, and a Global Positioning System (GPS). The telescope collects scattered sunlight that enters the spectrometer (Ocean Optics HR2000) through an optical fiber. The spectrometer, which is stored in a miniature refrigerator that has a stable temperature, has a spectral resolution of about 0.6 nm and a spectral range of 290 nm to 420 nm. The GPS tracks the coordinates of the measurement route as well as provides the car speed and acquisition time for each spectrum. A miniature weather station is fixed on the roof of the measurement van in order to record meteorological data such as wind speed, wind direction, temperature, humidity, and pressure along the route. The entire system is automatically controlled by our AIOFM mobile DOAS software (Li et al., 2005).

The Long-Path DOAS instrument used to explore the influence of GEA on the downwind region (see Sect. 3.4) uses a Xenon lamp as light source and a UV/VIS spectrometer (QE65000, Ocean Optics). The detailed setup of the Long-Path DOAS instrument has been provided by Qin et al. (2006). The instrument is mounted on the third floor (about 15 m above ground) of one of the buildings at Guangzhou University Town (Fig. 1), southeast of Guangzhou City, about 20 km away from GEA, with an optical path length of about 788 m. The wavelength coverage of this instrument, ranging from

Observations of SO₂ and NO₂ by mobile DOAS in Guangzhou Eastern Area

F. C. Wu et al.

Title Page

Abstract

Introduction

Conclusions

References

Tables

Figures

⏪

⏩

◀

▶

Back

Close

Full Screen / Esc

Printer-friendly Version

Interactive Discussion



260 nm to 369 nm, allows the monitoring of SO₂, HCHO, NO₂, and O₃ among others. During this campaign, the instrument is mainly used to monitor SO₂, NO₂, and O₃.

In this study, the MAX-DOAS instrument is used to obtain the vertical columns for NO₂ and SO₂. This system is also from the AIOFM, with parts such as a stepper motor used to rotate a telescope, a miniature spectrometer (Ocean Optics HR2000) with a spectral resolution of 0.6 nm and a miniature refrigerator to maintain a stable temperature. Scattered sunlight is collected and focused by the telescope and is led into the spectrometer unit through an optical fiber. This MAX-DOAS system is designed to adjust different viewing directions into a desired elevation angle sequentially observed at 5°, 10°, 20°, 30°, and 90° by a stepper motor. The detailed description of our MAX-DOAS system is given in Li et al. (2007b).

2.3 Description of OMI

The Ozone Monitoring Instrument (OMI) (Levelt et al., 2006) onboard the NASA Earth Observation System (EOS)-Aura satellite was launched on 15 June 2004. It is capable of monitoring global atmospheric NO₂ via observation of backscattered sunlight in the wavelength range of 270 to 500 nm. The crossing time for OMI is 13:45 LT (local time) on the ascending node. Compared with NO₂ satellite observations from GOME, GOME-2, and SCHIAMACHY, OMI can provide a dataset with higher spatial (13 × 24 km) and temporal resolution (daily global coverage). The OMI retrieval of NO₂ vertical columns based on the DOAS method and consists of three steps: determination of slant column densities, conversion to vertical column densities using the so-called air mass factor (AMF), and estimation of the stratospheric contribution. The detailed description of this retrieval process can be found in Bucselá et al. (2006).

Ground-based (Louisa et al., 2008) or airborne (Dix et al., 2009; Heue et al., 2011; Sluis et al., 2010) measurements cover a limited spatial area, where vertical column densities may not completely represent the whole spatial extent of the satellite ground pixel. Mobile DOAS observations, on the other hand, can provide more data points within a given satellite ground pixel and be used to detect the variability and gradients

Observations of SO₂ and NO₂ by mobile DOAS in Guangzhou Eastern Area

F. C. Wu et al.

Title Page

Abstract

Introduction

Conclusions

References

Tables

Figures

⏪

⏩

◀

▶

Back

Close

Full Screen / Esc

Printer-friendly Version

Interactive Discussion



Observations of SO₂ and NO₂ by mobile DOAS in Guangzhou Eastern Area

F. C. Wu et al.

Title Page

Abstract

Introduction

Conclusions

References

Tables

Figures

⏪

⏩

◀

▶

Back

Close

Full Screen / Esc

Printer-friendly Version

Interactive Discussion



(Wagner et al., 2010). In the current study, the OMI tropospheric NO₂ data product of NASA is used (Bucsela et al., 2006). To achieve a better comparison between OMI NO₂ and mobile DOAS data, the OMI tropospheric NO₂ VCDs are gridded onto a 0.1° × 0.1° grid (Wenig et al., 2008; Chan et al., 2012). The NO₂ VCDs are then compared with the corresponding OMI grid cell (113.50° E–113.75° E, 22.75° N–23.00° N).

2.4 Principle of mobile DOAS

2.4.1 Retrieval of vertical columns for tropospheric trace gases

The DOAS technique has been employed in numerous applications that use artificial light sources or sunlight with instruments mounted on various fixed or mobile platforms (see Platt and Stutz, 2008 for a comprehensive overview). The DOAS evaluation procedure is described in this section in relation to our mobile observation of sunlight intensities in a zenith viewing direction, and the retrieval of tropospheric SO₂ and NO₂ from these intensity spectra. Details of the DOAS analysis are presented in Platt and Stutz (2008).

The spectral evaluation applied to each recorded spectrum while the van moves along the measurement route starts with a dark current correction, followed by the division with a Fraunhofer reference spectrum. Subsequently, a high pass filter is applied to the logarithm of this ratio to separate the broad and narrow band spectral structures. Differential slant column densities (SCD, defined as the concentration integrated along the light path), i.e. amounts of trace gas relative to the reference, are then obtained by fitting narrow band spectral absorption cross sections to the processed measurement spectra. Figure 3 illustrates such a DOAS fit for NO₂ and SO₂ using the Windoas software package (Van Roozendaal et al., 2001) for mobile DOAS measurement.

During our retrieval process, a spectrum is first selected arbitrarily on the upwind path as the reference spectrum to obtain the concentration distribution trends along the route. The minimum concentration of SO₂ and NO₂ along each driving route is then chosen as the Fraunhofer spectra to re-retrieve the measurement spectra. The

VCDs using tropospheric differential air mass factors (DAMFs) according to the following formula:

$$\text{VCD}_{\text{trop}} = \frac{\text{DSCDs}}{\text{DAMF}}. \quad (1)$$

The radiative transfer model SCIATRAN (Rozanov et al., 2002) is used to calculate DAMFs under the assumption that aerosol and trace gas profiles are given by constant values below the boundary layer height and the exponential profiles above. The height of the boundary layer is deduced from LIDAR observations (Fig. 1) carried out by the AIOFM and was on average about 1.5 km during our measurements. For the radiative transfer calculations, aerosol extinction coefficients within the layer are taken from the LIDAR, while the NO₂ and SO₂ mixing ratios are obtained from the Long-path DOAS measurements. Aerosol and trace gas profiles above the boundary layer are sourced from the LOWTRAN database (Kneizys et al., 1988) and the US standard atmosphere (US Government Printing Office, 1976), respectively.

2.4.2 Emission calculation

The mobile DOAS measurement allows the emission from pollutant sources to be further quantified for known wind direction, wind speed, and car speed. The total SO₂ and NO₂ emissions from a source are determined using the following equation (Johansson et al., 2009; Ibrahim et al., 2010):

$$\text{Flux}_{\text{gas}} = \sum \text{VCD}_{\text{gas}} \cdot V_m \cdot V_{w_{\perp}} \cdot \Delta t \quad (2)$$

where VCD_{gas} is the vertical column density, V_m is the car speed, V_{w_⊥} is the component of wind speed perpendicular to the driving direction, and Δt is the time for acquiring one spectrum (i.e. integration time, about 9 s in this study). In this equation, the sum refers to all the measurement spectra along the path.

Observations of SO₂ and NO₂ by mobile DOAS in Guangzhou Eastern Area

F. C. Wu et al.

Title Page

Abstract

Introduction

Conclusions

References

Tables

Figures

⏪

⏩

◀

▶

Back

Close

Full Screen / Esc

Printer-friendly Version

Interactive Discussion



Wind direction and speed are taken from the miniature mobile weather station installed on the van. The car speed, location, and direction of each segment are from the GPS.

3 Results and discussion

3.1 Distribution of SO₂ and NO₂ around GEA

3.1.1 Identification of emission sources

In this section, the distributions of SO₂ and NO₂ vertical columns along the measurement path are analyzed following the results of the mobile DOAS data described in Sect. 2. The possible emission sources are discussed further using these distributions for different wind fields.

Figure 4 shows the resulting MAX-DOAS VCDs during the measurement period. Figure 4a, b also illustrates the mobile DOAS VCDs and the offsets between the two instruments. The average offsets of SO₂ and NO₂ are $5.72 \pm 1.49 \times 10^{15}$ molecules cm⁻² and $6.85 \pm 2.49 \times 10^{15}$ molecules cm⁻², respectively. An example result of SO₂ after SO₂ offset correction on 25 November is shown in Fig. 4c. Three peaks are also found in Fig. 4a and b. The peaks of SO₂ (peak1, peak2, peak3) are related to the strong emissions of pollutant sources under the northeasterly wind. The peaks of NO₂ (peak1 and peak2) on 11 and 29 November are presumably caused by the same pollutant source, but the peak on 21 December (peak3) may be related to the transport from other regions by the northwesterly wind.

Figure 5 shows the wind direction and wind speed during the whole experimental period. The wind mostly came from the north and northeast with the exception of 21, 27 November, 5, 13 December (southeast direction), 30 November and 21 December (northwest), and 4, 23 December (east). Average wind speed ranged from 1 to 5 m s⁻¹ during the measurement period. According to the distributions of SO₂ and NO₂ around

Observations of SO₂ and NO₂ by mobile DOAS in Guangzhou Eastern Area

F. C. Wu et al.

Title Page

Abstract

Introduction

Conclusions

References

Tables

Figures

⏪

⏩

◀

▶

Back

Close

Full Screen / Esc

Printer-friendly Version

Interactive Discussion



the path, four types of wind fields are distinguished in our study: north or northeast, southeast, east, and northwest.

Typical spatial distributions of SO₂ and NO₂ vertical columns around GEA for these four different wind fields are shown in Fig. 6. The maps for SO₂ in Fig. 6 show a peak in the north irrespective of wind direction, suggesting an additional emission source outside the GEA and north from it. The comparison for wind direction from north/northeast and east versus west further suggested that it is located in the northeast rather than the northwest. No such peak exists for NO₂ in the north if the wind is coming from the north, so that we infer an SO₂ source indeed lies in the northeast of GEA (source 1 in Fig. 7).

For the southeast wind, downwind peaks are found simultaneously for SO₂ and NO₂ in the northwest corner of our route (Fig. 6b). The corresponding downwind peaks for the reverse wind direction from the northwest are less pronounced, and thus sources of NO₂ and SO₂ within the encircled measurement area, but closer to the northern measurement route, can be identified (source 2 in Fig. 7). The location of peaks in the downwind region for the north and northeast wind (Fig. 6a and c) is consistent with this conjecture.

Increased values of NO₂ appeared for all wind directions in the southeast/south of the measurement route, especially on 29 November and 4 December. These high column densities can most likely be attributed to traffic emissions from Humen Bridge in the south of GEA (Fig. 7), the main channel from Shenzhen and Dongguan to Guangzhou. During the Asian Games, the Guangzhou government set up a security checkpoint here, which occasionally caused traffic jams that enhanced high NO₂ concentration.

3.1.2 Comparison with OMI NO₂

The comparison between NO₂ VCDs of the mobile DOAS and OMI for the ground pixel (113.50° E–113.75° E, 22.75° N–23.00° N), as specified in Sect. 2.3 during the Asian Games, is shown in Fig. 8. Our mobile DOAS values were higher than the OMI values most of the time, especially for the measurements from 27 November to 7 December.

Observations of SO₂ and NO₂ by mobile DOAS in Guangzhou Eastern Area

F. C. Wu et al.

Title Page

Abstract

Introduction

Conclusions

References

Tables

Figures

⏪

⏩

◀

▶

Back

Close

Full Screen / Esc

Printer-friendly Version

Interactive Discussion



Aside from the averaged value of OMI for large areas and its insensitivity to the near-surface pollutant sources, the influence of clouds was also considered and treated as a dominant factor for the OMI and mobile DOAS observations.

Cloud fractions for our 14 days of measurement (Table 1) varied considerably during the measurement period. A cloud fraction of 0.4 was used as threshold to filter both data for comparison. This fraction was exceeded on 21, 27, 29 November as well as 7, 9 December. Figure 9 shows the correlation between the two measurements for cloud fractions smaller than 0.4. The correlation coefficient (R^2) is 0.88, indicating that the relative changes observed in OMI and mobile DOAS were coincident.

Although both instruments agree in general, high NO_2 VCDs were likely underestimated by OMI while low NO_2 VCDs were likely overestimated. These discrepancies, however, cannot be simply attributed to clouds. For example, the 22 and 23 December cloud coverage was lower yet the discrepancies were higher with respect to those of the 11, 19, and 25 November cloud coverage. The disagreement between both data sets could also be caused by the different assumptions on the calculation of their air mass factors including different aerosol and trace gas profiles, ground albedo, etc. Furthermore, mobile and satellite measurements refer to slightly different times. The dependency on the NO_2 profile assumed for the AMF calculation is discussed by Chan et al. (2012) and Wang et al. (2012). In Fig. 10, the NO_2 surface concentrations were significantly enhanced on 22 and 23 December. The NO_2 VCDs from OMI were underestimated on 22 and 23 December. The comparison of spatial patterns in the two data sets in Fig. 11 shows that both mobile DOAS and OMI captured the high NO_2 VCDs in the northern and southern part of the mobile DOAS route (in the northern part due to industrial emissions, in the southern part due to vehicle emissions from the Humen Bridge) as well as low VCDs in the western part (white circles in Fig. 11).

Observations of SO_2 and NO_2 by mobile DOAS in Guangzhou Eastern Area

F. C. Wu et al.

Title Page

Abstract

Introduction

Conclusions

References

Tables

Figures

⏪

⏩

◀

▶

Back

Close

Full Screen / Esc

Printer-friendly Version

Interactive Discussion



3.2 Estimation of SO₂ and NO₂ emissions

3.2.1 Emission of SO₂ and NO₂ from GEA

As a key component in the estimation of SO₂ and NO₂ emissions, wind fields can be the source of large errors. Wind fields are generally used to estimate emissions about 400 m a.g.l. (according to the stack height of power plant and height of elevated plume as discussed by Mellqvist et al., 2007). A wind profile radar would provide highly accurate data. Such data, however, are not available for our measurements. Wind data from our mobile weather station are used instead. To minimize the error caused by the influence of surface processes on the wind field, the measurement days with relatively stable and constant vertical wind from ground to 400 m height are selected to estimate emissions. Figure 12 compares the wind direction (Fig. 12a) and wind speed (Fig. 12b) at 400 m height to the surface once every 14 days from 9 November to 22 December. The wind field at 400 m is taken from observations at Kings Park (station number: 45004, 114.16° E, 22.31° N) in Hong Kong, about 80 km southeast of GEA (<http://weather.uwyo.edu/upperair/sounding.html>). With few exceptions, the wind fields at both altitudes and locations generally agree.

The total emissions of SO₂ and NO₂ from the encircled area are estimated using Eq. (2). The estimated emissions of SO₂ and NO₂ from GEA for 14 days are shown in Fig. 13, with a fractional cloud cover lower than 0.4 and a stable wind field. The entire measurement period is divided into five phases: before the Asian Games (9 and 11 November, phase 1), during the Asian Games (15, 17, 19, and 23 November, phase 2), the time between the Asian Games and the Asian Para Games (2, 3, and 4 December, phase 3), during the Asian Para Games (13, 17, and 19 December, phase 4), and after the Games (21 and 22 December, phase 5). SO₂ emissions varied strongly between the different phases (by a factor of 5), where the lower and lowest emissions occurred during the Asian Games and Asian Para Games, respectively. A clear pattern for NO₂ emissions was not found, although these emissions decreased at the beginning of the Games and increased again after their end.

Observations of SO₂ and NO₂ by mobile DOAS in Guangzhou Eastern Area

F. C. Wu et al.

Title Page

Abstract

Introduction

Conclusions

References

Tables

Figures

⏪

⏩

◀

▶

Back

Close

Full Screen / Esc

Printer-friendly Version

Interactive Discussion



Observations of SO₂ and NO₂ by mobile DOAS in Guangzhou Eastern Area

F. C. Wu et al.

Title Page

Abstract

Introduction

Conclusions

References

Tables

Figures

⏪

⏩

◀

▶

Back

Close

Full Screen / Esc

Printer-friendly Version

Interactive Discussion



The reduced emission of SO₂ during the Asian Games and Asian Para Games could be caused mainly by the pollution control strategy of the local environmental protection agency. Meteorological conditions also play an important role for emissions from GEA. Persistent rainfall from 10 to 12 December and again from 14 to 16 December helped to remove air pollutants, thereby decreasing emissions from GEA during the Asian Para Games. Table 2 summarizes the average SO₂ emission for the different phases of the measurement period. For times outside the Games (phases 1, 3, and 5), SO₂ emission was estimated to be 9.50 tons per hour (approximately 83.2×10^3 tons per year), which is consistent with the value of 84.60×10^3 tons per year from the Guangzhou emission inventory (Guangzhou Municipality State of the Environment, 2010). On the other hand, the average NO₂ emission for this time was estimated to be 3.5 tons per hour. During the Games (including phases 2 and 4) the emissions of SO₂ and NO₂ were reduced by 53.5 and 46 %, respectively, compared with the time outside the Games (including phases 1, 3, and 5).

Errors in the calculation of emissions can be due to errors in the column retrieval, wind field, and car speed. The fitting error in the column retrieval was estimated to be less than 15 % for NO₂ and 20 % for SO₂ (Fig. 3). The error of car speed was about 1 % according to the GPS. In our study, the errors caused by uncertainties in the wind field were not determined. Mellqvist et al. (2007) estimated the errors to be as large as 30 %, and thus the error of total emissions is estimated to be about 33 % for NO₂ and 36 % for SO₂.

3.2.2 Influence of SO₂ emissions from the GEA on the downwind region

Knowledge of emissions and transportation from large area sources is crucial for the control and management of local environment problems. Guangzhou University Town (113.37° E, 23.05° N) hosted numerous events during the Asian Games, which raised issues on the air quality of the town. According to the geographical relationship between GEA and Guangzhou University Town from Fig. 1, the pollutants from GEA can diffuse to Guangzhou University Town when the wind direction is southeast or east. The SO₂

Observations of SO₂ and NO₂ by mobile DOAS in Guangzhou Eastern Area

F. C. Wu et al.

Title Page

Abstract

Introduction

Conclusions

References

Tables

Figures

⏪

⏩

◀

▶

Back

Close

Full Screen / Esc

Printer-friendly Version

Interactive Discussion

concentration in Guangzhou University Town is expected to increase due to the contribution of GEA emission. SO₂ is selected as the tracer gas because it originates from industrial emissions, unlike NO₂ which is still affected by local vehicle emissions. To investigate how emissions from GEA affect Guangzhou University Town for southeasterly winds, a long-path DOAS instrument is set up there to monitor possible downwind transport of SO₂.

The paths of air masses for southeasterly wind on 21 and 27 November, and 5 and 13 December are shown in Fig. 14. On these days, the wind traversed GEA and the SO₂ concentrations measured downwind at the University Town monitoring site based on our Long-path instrument, which were significantly higher as illustrated in Fig. 15 (shaded box). This is consistent with the observation by our mobile DOAS in Fig. 6b for the southeasterly wind. Wind from the southeast also occurred on 24 and 28 November and 10 (Fig. 16a) and 12 (Fig. 16b) December when we could not carry out mobile measurements due to traffic limitations. The SO₂ concentrations were also enhanced at the University Town monitoring site on these four days (Fig. 15).

Considering all these days, the average SO₂ concentrations for southeasterly and non-southeasterly winds measured by the Long-path DOAS at the downwind location are shown in Fig. 17. Daily averages of SO₂ are enhanced by a factor 3 when air masses traversed GEA, compared to days when the wind came from other directions. Therefore, GEA is concluded to be a major contributor to SO₂ pollution in the Guangzhou University Town area.

4 Conclusions

In this paper, mobile DOAS observations carried out in GEA during the Guangzhou Asian Games from November to December 2010 are reported. These measurements were used to investigate the spatial and temporal distributions of SO₂ and NO₂ around and emissions from GEA during the Asian Games period.

Observations of SO₂ and NO₂ by mobile DOAS in Guangzhou Eastern Area

F. C. Wu et al.

Title Page

Abstract

Introduction

Conclusions

References

Tables

Figures

⏪

⏩

◀

▶

Back

Close

Full Screen / Esc

Printer-friendly Version

Interactive Discussion

A MAX-DOAS instrument at a fixed location concurrently measured estimates of absolute vertical columns for NO₂ and SO₂ of the mobile DOAS measurements. The average offsets of SO₂ and NO₂ between the mobile DOAS and MAX-DOAS were $5.72 \pm 1.49 \times 10^{15}$ molecules cm⁻² and $6.85 \pm 2.49 \times 10^{15}$ molecules cm⁻², respectively.

Distributions of SO₂ and NO₂ vertical columns were obtained with help of the mobile DOAS system. High SO₂ values appeared in the northeast and northwest of our measurement path under north and southeast wind fields, respectively. High NO₂ values were found in the north and southeast of the measurement path with higher variability due to varying traffic emissions. Possible emission sources were determined to explain these distributions using the information from different wind fields. Pollutant sources in the northeast of GEA, outside the closed measurement route and sources in the north, within the area encircled were also identified. Our NO₂ vertical columns were compared with OMI data and were found to be similar in spatial patterns. The correlation coefficient (R^2) of the vertical columns after cloud filtering was 0.88, but the absolute values measured by our mobile DOAS were mostly higher than the OMI data. SO₂ and NO₂ emissions from the GEA during the Asian Games period were also calculated. Lower and lowest emissions of SO₂ were found to occur during the Asian Games and Asian Para Games, respectively. Outside the Asian Games period, the average emission of SO₂ was estimated to be 9.50 ± 0.90 tons per hour (83.2 thousand tons per year), which is consistent with the value of 84.6 thousand tons per year from a local emission inventory. In comparison, the average emission of NO₂ was estimated to be 3.50 ± 1.89 tons per hour. During the Games, the emissions of SO₂ and NO₂ were reduced by 53.50 and 46 %, respectively. The error of total emissions was estimated to be about 33 % for NO₂ and 36 % for SO₂. Using LP-DOAS measurements at the Guangzhou University Town, emissions from GEA were found to have a distinct impact on air pollution in this area depending on the wind direction; SO₂ concentrations were found to be about three times larger during our measurements when air masses crossed GEA.

Acknowledgements. The authors would like to thank the Guangzhou Environmental Center for supporting the experiment. We also want to thank our two drivers, Shaoli Wang and Zongmao Xu, whose skillful driving ensured that the experiment could be carried out successfully and safely. This work was also made possible by the support of Special research funding for the public industry sponsored by Ministry of Environmental Protection of PRC (Grant No: 201109007) and the National Natural Science Foundation of China 40905010, 41275038.

References

- Bogumil, K., Orphal, J., Homann, T., Voigt, S., Spietz, P., Fleischmann, O. C., Vogel, A., Hartmann, M., Kromminga, H., Bovensmann, H., Frerick, J., and Burrows, J. P.: Measurements of molecular absorption spectra with the SCIAMACHY pre-flight model: instrument characterization and reference data for atmospheric remote-sensing in the 230–2380 nm region, *J. Photoch. Photobio. A*, 157, 167–184, 2003.
- Bucsela, E., Celarier, E., Wenig, M., Gleason, J., Veefkind, P., Boersma, K., and Brinksma, E.: Algorithm for NO₂ vertical column retrieval from the Ozone Monitoring Instrument, *IEEE T. Geosci. Remote*, 44, 1245–1258, 2006.
- Cao, J. J., Lee, S. C., Ho, K. F., Zou, S. C., Fung, K., Li, Y., Watson, J. G., and Chow, J. C.: Spatial and seasonal variations of atmospheric organic carbon and elemental carbon in Pearl River Delta Region, China, *Atmos. Environ.*, 38, 4447–4456, 2004.
- Chan, K. L., Pöhler, D., Kuhlmann, G., Hartl, A., Platt, U., and Wenig, M. O.: NO₂ measurements in Hong Kong using LED based long path differential optical absorption spectroscopy, *Atmos. Meas. Tech.*, 5, 901–912, doi:10.5194/amt-5-901-2012, 2012.
- Dix, B., Brenninkmeijer, C. A. M., Frieß, U., Wagner, T., and Platt, U.: Airborne multi-axis DOAS measurements of atmospheric trace gases on CARIBIC long-distance flights, *Atmos. Meas. Tech.*, 2, 639–652, doi:10.5194/amt-2-639-2009, 2009.
- Edner, H., Ragnarson, P., Svanberg, S., Wallinder, E., Ferrara, R., Cioni, R., Raco, B., and Taddeucci, G.: Total fluxes of sulfur dioxide from the Italian volcanoes Etna, Stromboli, and Vulcano measured by differential absorption lidar and passive differential optical absorption spectroscopy, *J. Geophys. Res.*, 99, 18827–18838, 1994.
- Finlayson-Pitts, B. J. and Pitts, J. N.: *Chemistry of the Upper and Lower Atmosphere: Theory, Experiments, and Applications*, Academic Press, San Diego, USA, 1999.

Observations of SO₂ and NO₂ by mobile DOAS in Guangzhou Eastern Area

F. C. Wu et al.

Title Page

Abstract

Introduction

Conclusions

References

Tables

Figures

⏪

⏩

◀

▶

Back

Close

Full Screen / Esc

Printer-friendly Version

Interactive Discussion



Observations of SO₂ and NO₂ by mobile DOAS in Guangzhou Eastern Area

F. C. Wu et al.

Title Page

Abstract

Introduction

Conclusions

References

Tables

Figures

⏪

⏩

◀

▶

Back

Close

Full Screen / Esc

Printer-friendly Version

Interactive Discussion



- Kraus, S.: DOASIS, A Framework Design for DOAS, PhD-thesis, University of Mannheim, Shaker Verlag, Heidelberg, Germany, 2006.
- Kurucz, R. L., Furenlid, I., Brault, J., and Testerman, L.: Solar flux atlas from 296 nm to 1300 nm, National Solar Observatory Atlas No. 1, Office of University publisher, Harvard University, Cambridge, 1984.
- Levelt, P. F., van den Oord, G. H. J., and Dobber, M. R.: The ozone monitoring instrument, IEEE Trans. Geosci. Remote, 44, 1093–1101, 2006.
- Li, A., Liu, C., Xie, P. H., Liu, J. G., Qin, M., Dou, K., Fang, W., and Liu, W. Q.: Monitoring of SO₂ emissions from industry by passive DOAS, Proc. SPIE, 5832, 0277-786X/05/\$15, doi:10.1117/12.619651, 2005.
- Li, A., Xie, P. H., and Liu, W. Q.: Monitoring of total emission volume from pollution sources based on passive differential optical absorption spectroscopy, Acta Opt. Sin., 27, 1537–1542, 2007a.
- Li, A., Xie P. H., Liu, C., Liu J. G., and Liu W. Q.: A scanning multi-axis differential optical absorption spectroscopy system for measurement of tropospheric NO₂ in Beijing, Chin. Phys. Lett., 24, 2859–2862, 2007b.
- Louisa, J. K., Roland, J. L., John, J. R., and Paul, S. M.: Comparison of OMI and ground-based in situ and MAX-DOAS measurements of tropospheric nitrogen dioxide in an urban area, J. Geophys. Res., 113, D16S39, doi:10.1029/2007JD009168, 2008.
- Melamed, M. L., Basaldud, R., Steinbrecher, R., Emeis, S., Ruíz-Suárez, L. G., and Grutter, M.: Detection of pollution transport events southeast of Mexico City using ground-based visible spectroscopy measurements of nitrogen dioxide, Atmos. Chem. Phys., 9, 4827–4840, doi:10.5194/acp-9-4827-2009, 2009.
- Mellqvist, J., Samuelsson, J., and Rivera, C.: Measurements of industrial emissions of VOCs, NH₃, SO₂ and NO₂ in Texas using the solar occultation flux method and mobile DOAS, Final Report HARC Project H-53, Radio and Space Science Chalmers University of Technology, Göteborg, Sweden, 2007.
- Platt, U. and Stutz, J.: Differential Optical Absorption Spectroscopy: Principles and Applications, Springer, Heidelberg, Germany, 2008.
- Qin, M., Xie, P. H., Liu, W. Q., Li, A., Dou, K., Fang, W., Liu, H. G., and Zhang, W. J.: Observation of atmospheric nitrous acid with DOAS in Beijing, J. Environ. Sci.-China, 18, 69–75, 2006.

Observations of SO₂ and NO₂ by mobile DOAS in Guangzhou Eastern Area

F. C. Wu et al.

Title Page

Abstract

Introduction

Conclusions

References

Tables

Figures

◀

▶

◀

▶

Back

Close

Full Screen / Esc

Printer-friendly Version

Interactive Discussion



Rivera, C., Sosa, G., Wöhrnschimmel, H., de Foy, B., Johansson, M., and Galle, B.: Tula industrial complex (Mexico) emissions of SO₂ and NO₂ during the MCMA 2006 field campaign using a mobile mini-DOAS system, *Atmos. Chem. Phys.*, 9, 6351–6361, doi:10.5194/acp-9-6351-2009, 2009.

5 Rozanov, V. V., Buchwitz, M., Eichmann, K. U., de Beek, R., and Burrows, J. P.: Sciatran – a new radiative transfer model for geophysical applications in the 240–2400 nm spectral region: the pseudo-spherical version, *Adv. Space Res.*, 29, 1831–1835, 2002.

Shaiganfar, R., Beirle, S., Sharma, M., Chauhan, A., Singh, R. P., and Wagner, T.: Estimation of NO_x emissions from Delhi using Car MAX-DOAS observations and comparison with
10 OMI satellite data, *Atmos. Chem. Phys.*, 11, 10871–10887, doi:10.5194/acp-11-10871-2011, 2011.

Sluis, W. W., Allaart, M. A. F., Peters, A. J. M., and Gast, L. F. L.: The development of a nitrogen dioxide sonde, *Atmos. Meas. Tech.*, 3, 1753–1762, doi:10.5194/amt-3-1753-2010, 2010.

Takashima, H., Irie, H., Kanaya, Y., and Akimoto, H.: Enhanced NO₂ at Okinawa Island, Japan caused by rapid air-mass transport from China as observed by MAX-DOAS, *Atmos. Environ.*,
15 45, 2593–2597, 2011.

US government printing office: US Standard Atmosphere, 1976, Washington, DC, October 1976.

Van Roozendael, C. F.: WinDOAS 2.1 Software User Manual, IASB/BIRA, Brussel, Belgium, 2001.
20

Wagner, T., Ibrahim, O., Shaiganfar, R., and Platt, U.: Mobile MAX-DOAS observations of tropospheric trace gases, *Atmos. Meas. Tech.*, 3, 129–140, doi:10.5194/amt-3-129-2010, 2010.

Wang, W., Ren, L. H., Zhang, Y. H., Chen, J. H., Liu, H. J., Bao, L. F., Fan, S. J., and Tang, D. D.: Aircraft measurements of gaseous pollutants and particulate matter over Pearl River Delta in China, *Atmos. Environ.*, 42, 6187–6202, 2008.
25

Wenig, M. O., Cede, A. M., Bucsela, E. J., Celarier, E. A., Boersma, K. F., Veeffkind, J. P., Brinksma, E. J., Gleason, J. F., and Herman, J. R.: Validation of OMI tropospheric NO₂ column densities using direct-sun mode Brewer measurements at NASA Goddard Space Flight Center, *J. Geophys. Res.*, 133, D16S45, doi:10.1029/2007JD008988, 2008.

30 World Health Organization: WHO Air quality guidelines for particulate matter, ozone, nitrogen dioxide and sulfur dioxide Global update 2005 summary of risk assessment, Geneva, Switzerland, 2006.

Observations of SO₂ and NO₂ by mobile DOAS in Guangzhou Eastern Area

F. C. Wu et al.

Title Page

Abstract

Introduction

Conclusions

References

Tables

Figures

⏪

⏩

◀

▶

Back

Close

Full Screen / Esc

Printer-friendly Version

Interactive Discussion



- Wu, F. C., Xie, P. H., Li, A., Si, F. Q., Wang, Y., and Liu, W. Q.: Correction of the impact of multi scattering on NO₂ emission flux during the pollutants source measurement by mobile differential optical absorption spectroscopy, *Acta Opt. Sin.*, 31, 1101003-1–1101003-6, doi:10.3788/AOS201131.1101003, 2011.
- 5 Xu, J., Xie, P. H., Si, F. Q., Dou, K., Li, A., Liu, Y., and Liu, W. Q.: Retrieval of tropospheric NO₂ by multi axis differential optical absorption spectroscopy, *Spectrosc. Spect. Anal.*, 30, 2464–2469, 2010.
- Zhang, Q., David, G. S., He, K. B., Wang, Y. X., Richter, A., Burrows, J. P., Uno, I., Jang, C. J., Chen, D., Yao, Z. L., and Lei, Y.: NO_x emission trends for China, 1995–
10 2004: the view from the ground and the view from space, *J. Geophys. Res.*, 112, D22306, doi:10.1029/2007JD008684, 2007.
- Zhang, Y. H., Hu, M., Zhong, L. J., Wiedensohler, A., Liu, S. C., Andreae, M. O., Wang, W., and Fang, S. J.: Regional integrated experiments on air quality over Pearl River Delta 2004 (PRIDE-PRD2004): overview, *Atmos. Environ.*, 42, 6157–6173, 2008a.
- 15 Zhang, Y. H., Hu, M., and Wiedensohler, A.: The special issue on PRIDE-PRD 2004 campaign, *Atmos. Environ.*, 42, 6155–6156, 2008b.
- Zheng, J. Y., Zhang, L. J., Che, W. W., Zheng, Z. Y., and Yin, S. S.: A highly resolved temporal and spatial air pollutant emission inventory for the Pearl River Delta region, China and its uncertainty assessment, *Atmos. Environ.*, 43, 5112–5122, 2009.

Observations of SO₂ and NO₂ by mobile DOAS in Guangzhou Eastern Area

F. C. Wu et al.

Title Page

Abstract

Introduction

Conclusions

References

Tables

Figures

◀

▶

◀

▶

Back

Close

Full Screen / Esc

Printer-friendly Version

Interactive Discussion

Table 1. Cloud fraction for the 14 days of measurement. Italic text represents the cloud fraction < 0.4. Bold text represents the cloud fraction > 0.4. Cloud fractions are taken from the OMI data product.

Date	Cloud fraction
<i>9 Nov</i>	0.24
<i>11 Nov</i>	0.20
<i>13 Nov</i>	0.37
<i>19 Nov</i>	0.11
<i>25 Nov</i>	0.15
<i>2 Dec</i>	0.25
<i>21 Dec</i>	0.18
<i>22 Dec</i>	0.06
<i>23 Dec</i>	0.01
21 Nov	0.66
27 Nov	0.56
29 Nov	0.41
7 Dec	0.63
9 Dec	0.50

Observations of SO₂ and NO₂ by mobile DOAS in Guangzhou Eastern Area

F. C. Wu et al.

Title Page

Abstract

Introduction

Conclusions

References

Tables

Figures

⏪

⏩

◀

▶

Back

Close

Full Screen / Esc

Printer-friendly Version

Interactive Discussion

Table 2. SO₂ and NO₂ emissions as measured by our mobile DOAS for the different phases described in the text.

	Emission [th ⁻¹]					
	Phase 1	Phase 2	Phase 3	Phase 4	Phase 5	Phase 1 + 3 + 5
SO ₂	9.39 ± 1.06	6.38 ± 0.72	9.93 ± 0.15	2.45 ± 0.15	8.97 ± 1.58	9.50 ± 0.90
NO ₂	4.59 ± 1.35	2.14 ± 0.71	1.76 ± 0.44	1.64 ± 0.35	5.03 ± 1.73	3.50 ± 1.89

Observations of SO₂ and NO₂ by mobile DOAS in Guangzhou Eastern Area

F. C. Wu et al.

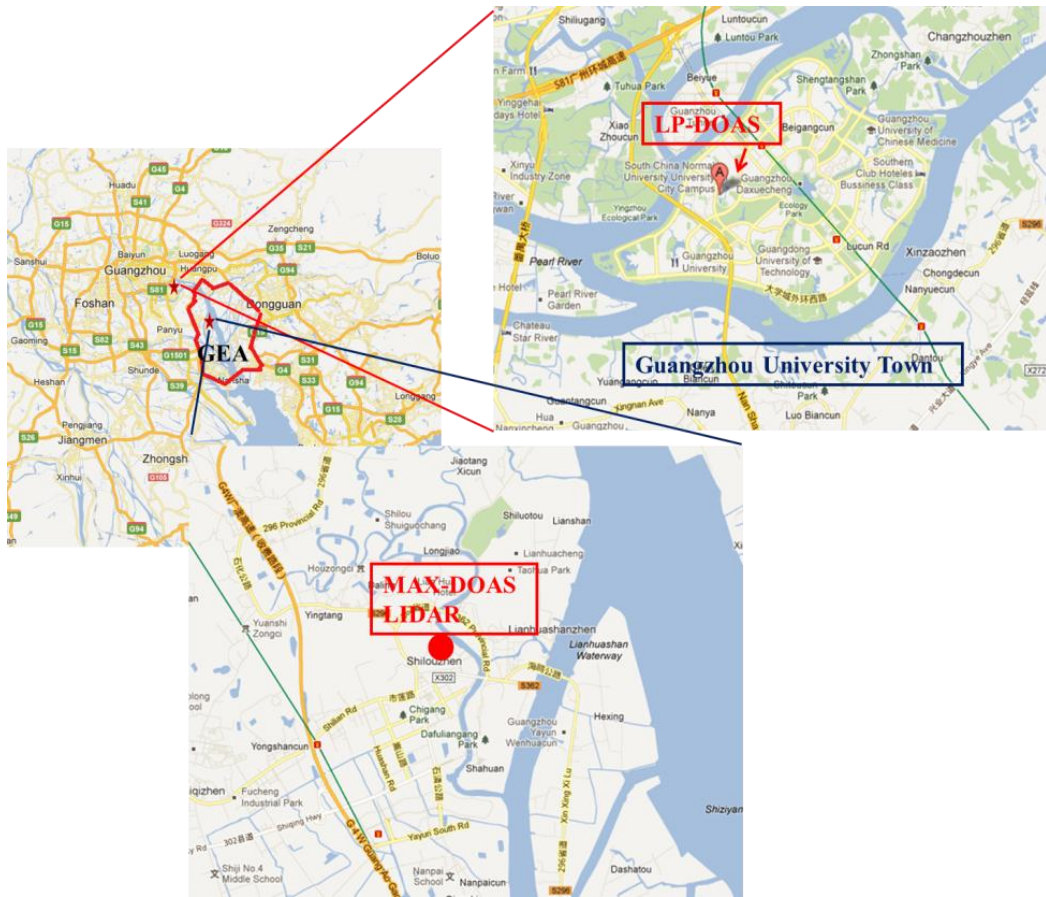


Fig. 1. Location of the Guangzhou Eastern Area (GEA). The mobile DOAS measurement path encircling this area is indicated by the closed red line. The locations of the LP-DOAS, MAX-DOAS, and Lidar instrument operated by the AIOFM are also shown.

Title Page

Abstract

Introduction

Conclusions

References

Tables

Figures

◀

▶

◀

▶

Back

Close

Full Screen / Esc

Printer-friendly Version

Interactive Discussion

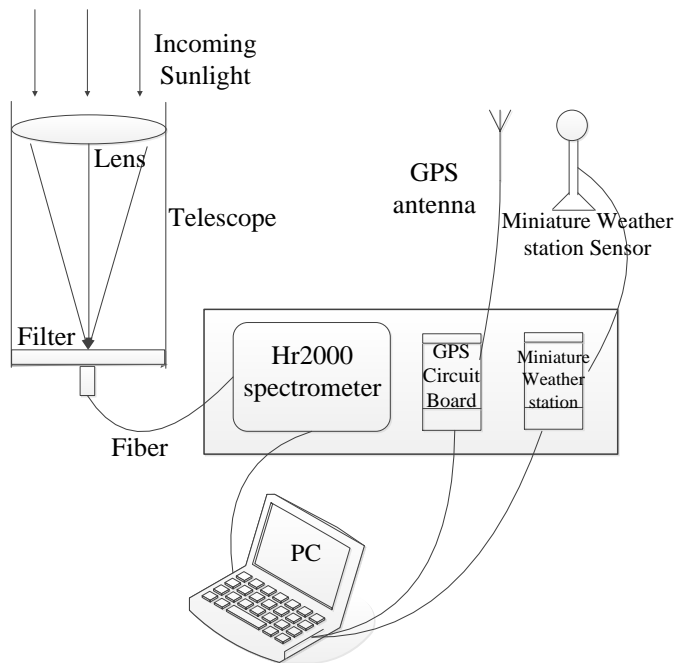


Fig. 2. Schematic diagram of the mobile DOAS instrument

Observations of SO₂ and NO₂ by mobile DOAS in Guangzhou Eastern Area

F. C. Wu et al.

Title Page

Abstract Introduction

Conclusions References

Tables Figures

⏪ ⏩

⏴ ⏵

Back Close

Full Screen / Esc

Printer-friendly Version

Interactive Discussion

Observations of SO₂ and NO₂ by mobile DOAS in Guangzhou Eastern Area

F. C. Wu et al.

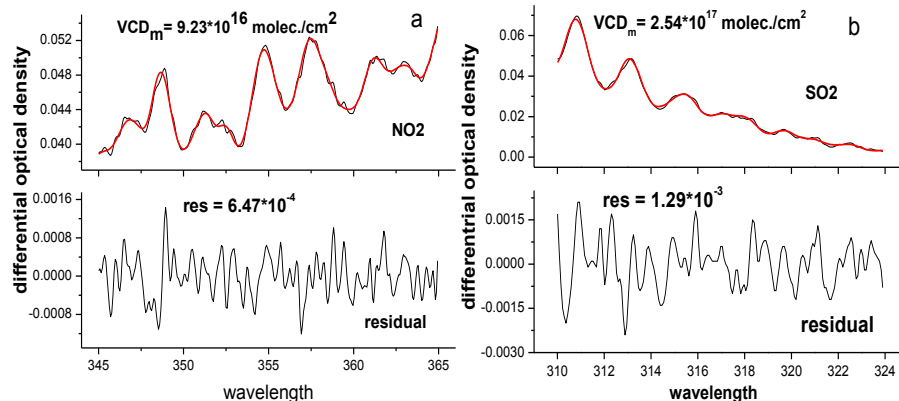


Fig. 3. Example fit for NO₂ (a) and SO₂ (b) recorded at 10:42 LT on 27 November 2010 and 10:35 LT on 29 November 2010 by our mobile DOAS instrument. Black lines denote the differential optical densities (DODs) of processed measurement spectra. Red lines show the result of the fit. The number given by VCD_m is the differential VCD with respect to the Fraunhofer reference spectrum as described in the text.

Observations of SO₂ and NO₂ by mobile DOAS in Guangzhou Eastern Area

F. C. Wu et al.

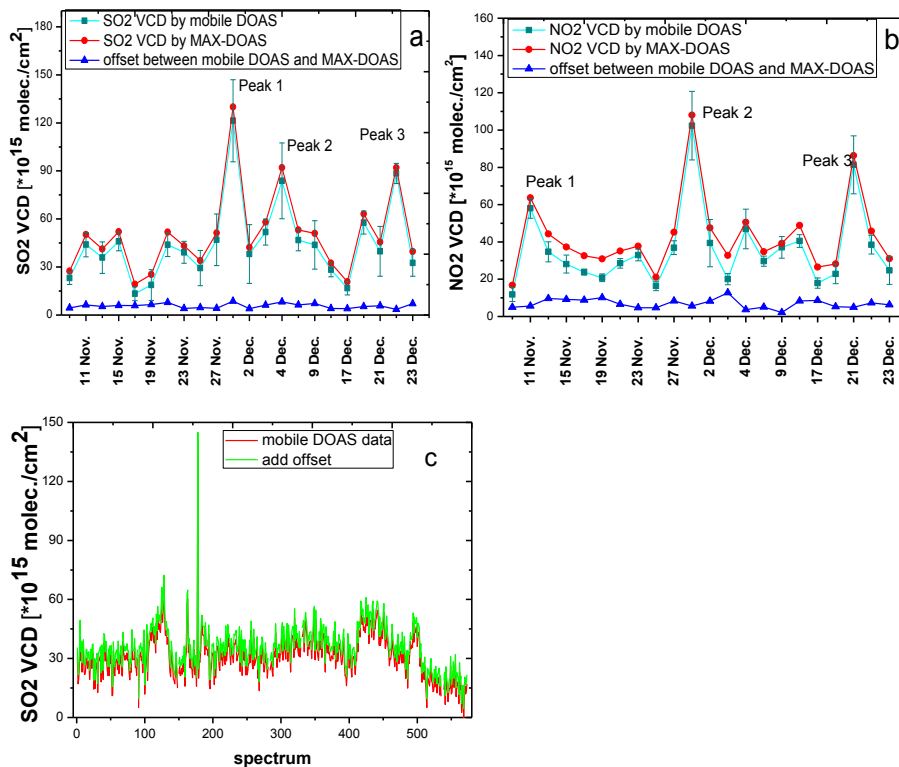


Fig. 4. Offset between MAX-DOAS and mobile DOAS values defined as the difference between these values for the measurement period for SO₂ (a) and NO₂ (b). The panel (c) shows the example for SO₂ on 25 November 2010. Red line: Original value from mobile DOAS, green line: result after adding the offset. Error bars indicate the standard deviation of mobile DOAS.

Observations of SO₂ and NO₂ by mobile DOAS in Guangzhou Eastern Area

F. C. Wu et al.

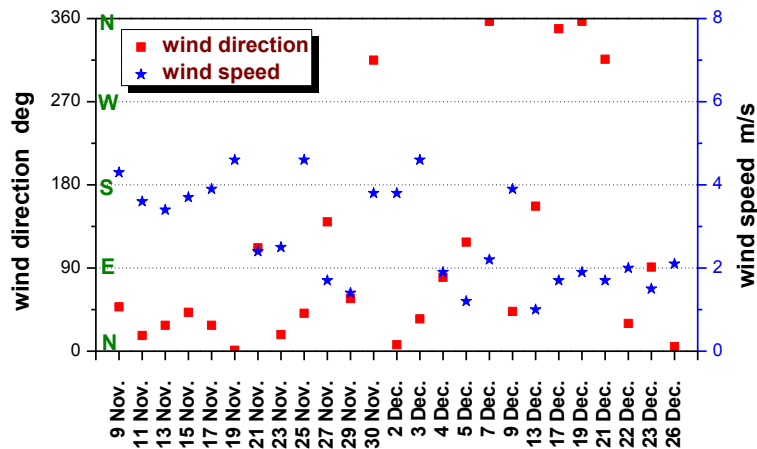


Fig. 5. Time series of average wind direction and wind speed during the measurement period recorded by our mobile miniature weather station.

Title Page

Abstract

Introduction

Conclusions

References

Tables

Figures

⏪

⏩

◀

▶

Back

Close

Full Screen / Esc

Printer-friendly Version

Interactive Discussion

Observations of SO₂ and NO₂ by mobile DOAS in Guangzhou Eastern Area

F. C. Wu et al.

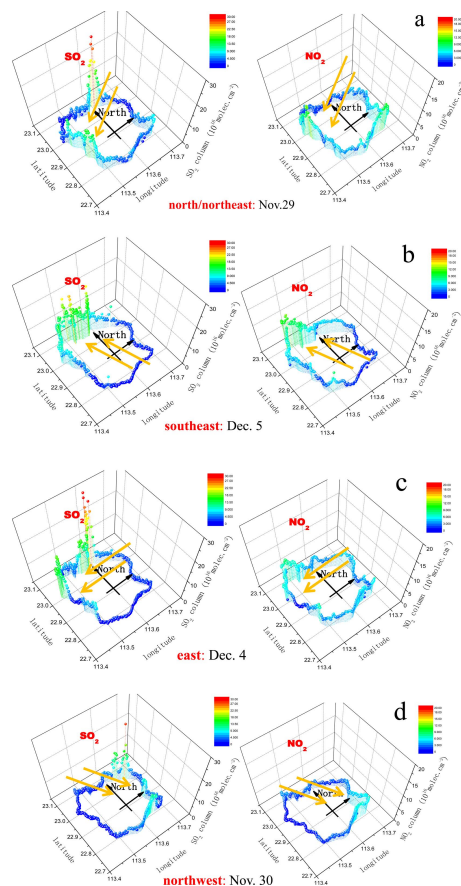


Fig. 6. Examples of SO₂ and NO₂ vertical columns (units: 10¹⁶ molecules cm⁻²) along the measurement path of the mobile DOAS for four typical wind directions: northeast/north (**a**), southeast (**b**), east (**c**), and northwest (**d**). Arrows indicate the average wind direction.

[Title Page](#)
[Abstract](#)
[Introduction](#)
[Conclusions](#)
[References](#)
[Tables](#)
[Figures](#)
[Back](#)
[Close](#)
[Full Screen / Esc](#)
[Printer-friendly Version](#)
[Interactive Discussion](#)

Observations of SO₂ and NO₂ by mobile DOAS in Guangzhou Eastern Area

F. C. Wu et al.

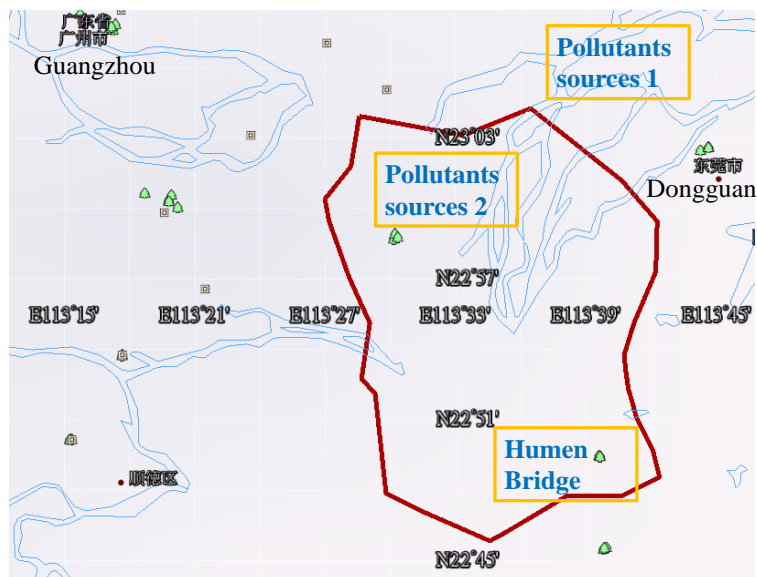


Fig. 7. Location of pollutant sources identified from the distributions of SO₂ and NO₂ vertical columns under different wind fields. The closed red line indicates the mobile DOAS measurement path.

Title Page

Abstract

Introduction

Conclusions

References

Tables

Figures

◀

▶

◀

▶

Back

Close

Full Screen / Esc

Printer-friendly Version

Interactive Discussion



Observations of SO₂ and NO₂ by mobile DOAS in Guangzhou Eastern Area

F. C. Wu et al.

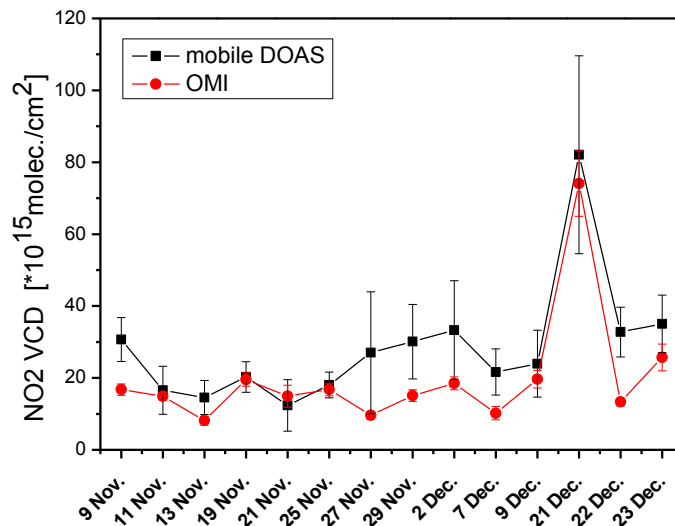


Fig. 8. Time series of NO₂ VCDs measured by mobile DOAS (black symbols) and OMI (red symbols). The bars show the standard deviations of OMI and mobile DOAS for NO₂ concentrations.

Title Page

Abstract

Introduction

Conclusions

References

Tables

Figures

⏪

⏩

◀

▶

Back

Close

Full Screen / Esc

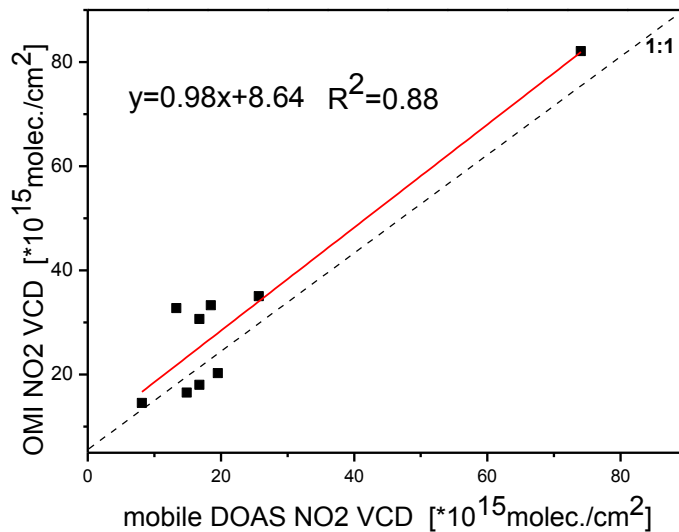
Printer-friendly Version

Interactive Discussion



**Observations of SO₂
and NO₂ by mobile
DOAS in Guangzhou
Eastern Area**

F. C. Wu et al.

**Fig. 9.** Correlation between the OMI and mobile DOAS NO₂ VCDs after cloud filtering.

Title Page

Abstract

Introduction

Conclusions

References

Tables

Figures

◀

▶

◀

▶

Back

Close

Full Screen / Esc

Printer-friendly Version

Interactive Discussion



**Observations of SO₂
and NO₂ by mobile
DOAS in Guangzhou
Eastern Area**

F. C. Wu et al.

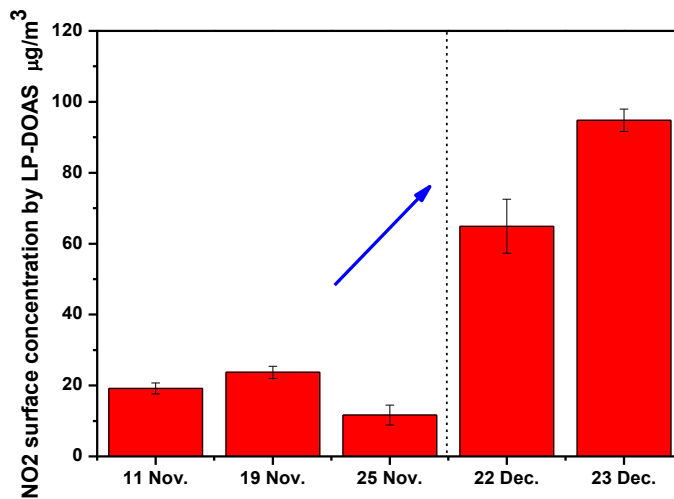


Fig. 10. NO₂ surface concentrations observed by LP-DOAS. The bars show the standard deviations of NO₂ concentrations from LP-DOAS during the mobile DOAS measurement time on 11, 19, and 25 November and 22 and 23 December.

[Title Page](#)[Abstract](#)[Introduction](#)[Conclusions](#)[References](#)[Tables](#)[Figures](#)[⏪](#)[⏩](#)[◀](#)[▶](#)[Back](#)[Close](#)[Full Screen / Esc](#)[Printer-friendly Version](#)[Interactive Discussion](#)

Observations of SO₂ and NO₂ by mobile DOAS in Guangzhou Eastern Area

F. C. Wu et al.

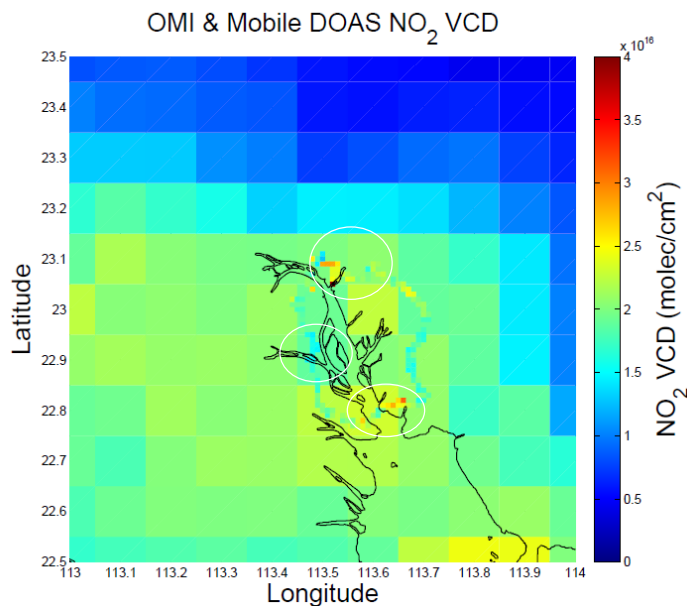


Fig. 11. Comparison of NO₂ VCD patterns measured from mobile DOAS and OMI during the whole measurement period (9 November to 23 December 2010). The large circle indicates the mobile DOAS observations. The white circles in the northern and southern part show the high NO₂ concentration captured by the two instruments. The white circle in the western part demonstrates the low NO₂ concentration. The grid resolution is 0.1° × 0.1°.

[Title Page](#)[Abstract](#)[Introduction](#)[Conclusions](#)[References](#)[Tables](#)[Figures](#)[◀](#)[▶](#)[◀](#)[▶](#)[Back](#)[Close](#)[Full Screen / Esc](#)[Printer-friendly Version](#)[Interactive Discussion](#)

Observations of SO₂ and NO₂ by mobile DOAS in Guangzhou Eastern Area

F. C. Wu et al.

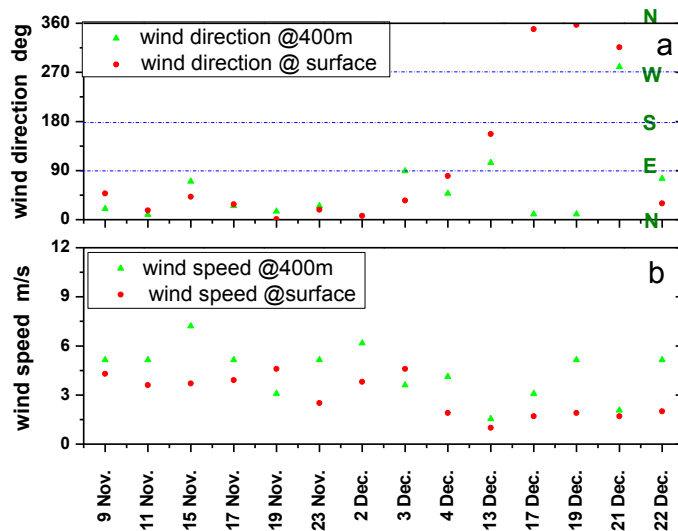


Fig. 12. Comparison of wind direction (a) and wind speed (b) at surface and 400 m height. The surface wind fields are from the mobile weather station. The wind fields at 400 m height are from (<http://weather.uwyo.edu/upperair/sounding.html>).

Title Page

Abstract Introduction

Conclusions References

Tables Figures

◀ ▶

◀ ▶

Back Close

Full Screen / Esc

Printer-friendly Version

Interactive Discussion



Observations of SO₂ and NO₂ by mobile DOAS in Guangzhou Eastern Area

F. C. Wu et al.

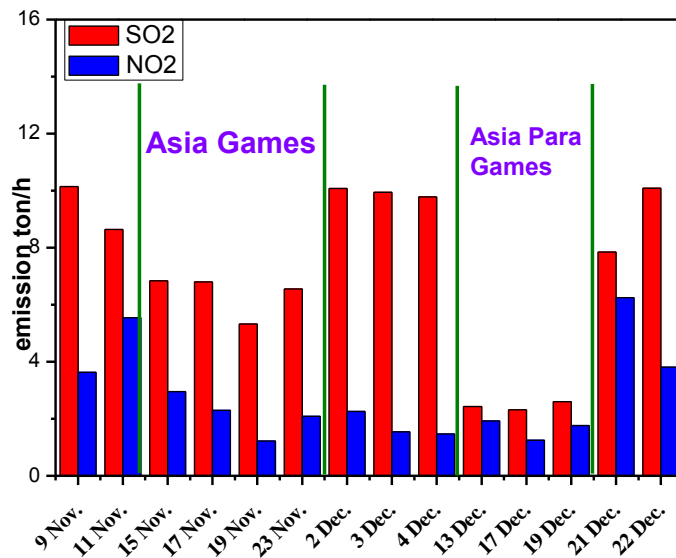


Fig. 13. SO₂ and NO₂ emissions estimated from mobile DOAS measurements. Green lines indicate the beginning and end of the Asian and Asian Para Games.

Title Page

Abstract

Introduction

Conclusions

References

Tables

Figures

⏪

⏩

◀

▶

Back

Close

Full Screen / Esc

Printer-friendly Version

Interactive Discussion



Observations of SO₂ and NO₂ by mobile DOAS in Guangzhou Eastern Area

F. C. Wu et al.

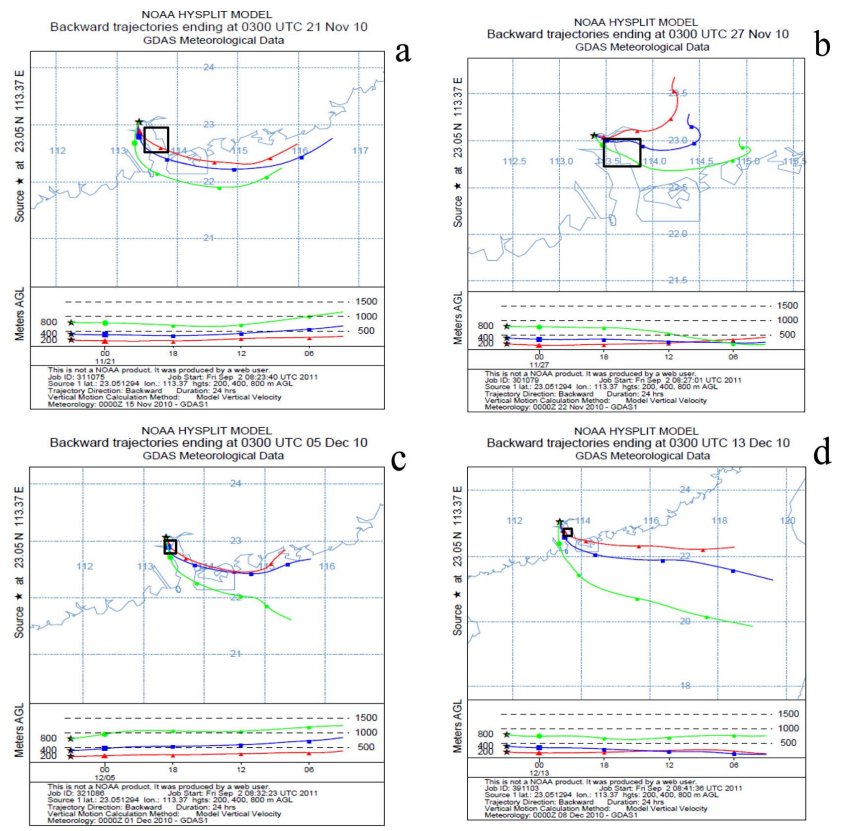


Fig. 14. Backward wind trajectories for the 200 m (red), 400 m (blue), and 800 m (green) heights at the Guangzhou University Town monitoring site from the NOAA HYSPLIT model (<http://www.arl.noaa.gov/index.php>) on 21 (a) and 27 (b) November, 5 (c) and 13 (d) December. The star indicates the Guangzhou University Town monitoring site, the black box measurement area of the mobile DOAS measurement.

Title Page

Abstract Introduction

Conclusions References

Tables Figures

⏪ ⏩

⏴ ⏵

Back Close

Full Screen / Esc

Printer-friendly Version

Interactive Discussion



Observations of SO₂ and NO₂ by mobile DOAS in Guangzhou Eastern Area

F. C. Wu et al.

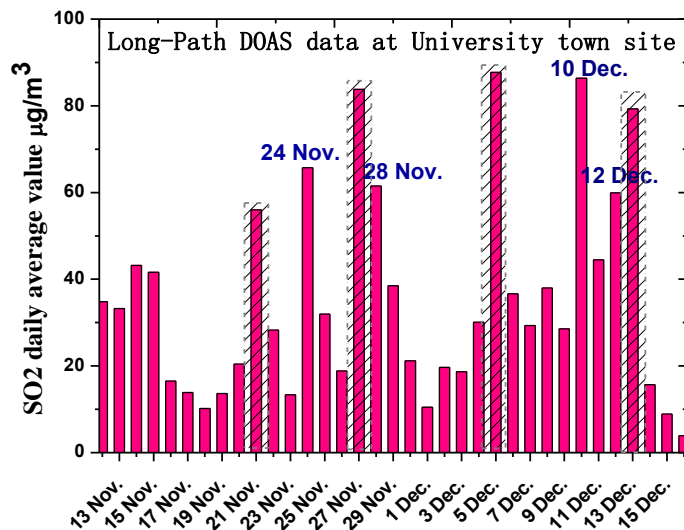
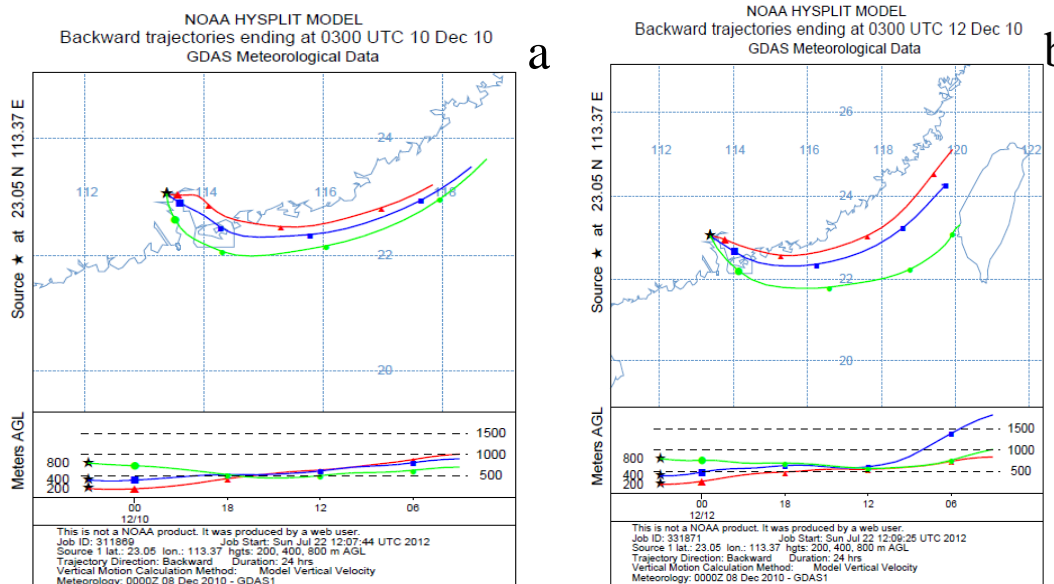


Fig. 15. Daily average SO₂ concentrations measured by Long-Path DOAS at the Guangzhou University Town site.

Observations of SO₂ and NO₂ by mobile DOAS in Guangzhou Eastern Area

F. C. Wu et al.



a

b

Fig. 16. Example of backward wind trajectories on 10 (a) and 12 (b) December. The element descriptions are the same as in Fig. 14.

Title Page

Abstract Introduction

Conclusions References

Tables Figures

⏪ ⏩

⏴ ⏵

Back Close

Full Screen / Esc

Printer-friendly Version

Interactive Discussion



Observations of SO₂ and NO₂ by mobile DOAS in Guangzhou Eastern Area

F. C. Wu et al.

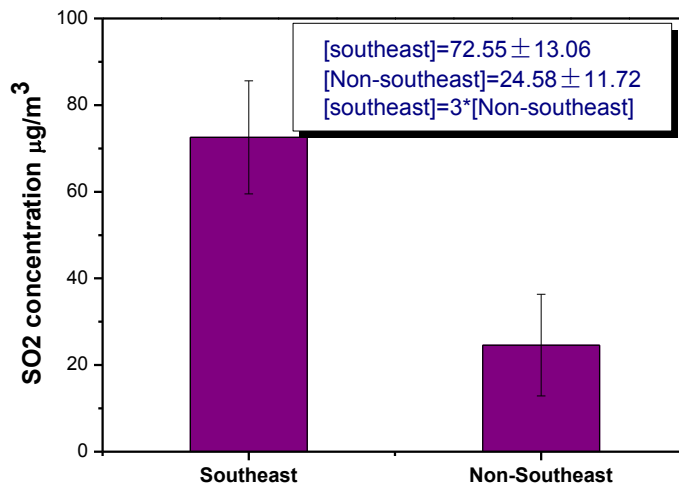


Fig. 17. Daily averaged SO₂ concentrations measured by our LP-DOAS at Guangzhou University Town site under the southeasterly and non-southeasterly winds.

Title Page

Abstract

Introduction

Conclusions

References

Tables

Figures

⏪

⏩

◀

▶

Back

Close

Full Screen / Esc

Printer-friendly Version

Interactive Discussion

